Distinct repriming and closed-state inactivation kinetics of Na$_v$1.6 and Na$_v$1.7 sodium channels in mouse spinal sensory neurons

Raimund I. Herzog, Theodore R. Cummins, Farshid Ghassemi, Sulayman D. Dib-Hajj and Stephen G. Waxman

Department of Neurology and PVA/EPVA Neuroscience Research Center, Yale Medical School, New Haven, CT 06510 and Rehabilitation Research Center, VA Connecticut Healthcare Center, West Haven, CT 06516, USA

While large, myelinated dorsal root ganglion (DRG) neurons are capable of firing at high frequencies, small unmyelinated DRG neurons typically display much lower maximum firing frequencies. However, the molecular basis for this difference has not been delineated. Because the sodium currents in large DRG neurons exhibit rapid repriming (recovery from inactivation) kinetics and the sodium currents in small DRG neurons exhibit predominantly slow repriming kinetics, it has been proposed that differences in sodium channels might contribute to the determination of repetitive firing properties in DRG neurons. A recent study demonstrated that Na$_v$1.7 expression is negatively correlated with conduction velocity and DRG cell size, while the Na$_v$1.6 voltage-gated sodium channel has been implicated as the predominant isoform present at nodes of Ranvier of myelinated fibres. Therefore we characterized and compared the functional properties, including repriming, of recombinant Na$_v$1.6 and Na$_v$1.7 channels expressed in mouse DRG neurons. Both Na$_v$1.6 and Na$_v$1.7 channels generated fast-activating and fast-inactivating currents. However recovery from inactivation was significantly faster (~5-fold at −70 mV) for Na$_v$1.6 currents than for Na$_v$1.7 currents. The recovery from inactivation of Na$_v$1.6 channels was also much faster than that of native tetrodotoxin-sensitive sodium currents recorded from small spinal sensory neurons, but similar to that of tetrodotoxin-sensitive sodium currents recorded from large spinal sensory neurons. Development of closed-state inactivation was also much faster for Na$_v$1.6 currents than for Na$_v$1.7 currents. Our results indicate that the firing properties of DRG neurons can be tuned by regulating expression of different sodium channel isoforms that have distinct repriming and closed-state inactivation kinetics.

Primary sensory neurons convey a broad range of sensory information from the periphery to the CNS and different subpopulations exhibit distinct electrophysiological properties. While large myelinated dorsal root ganglion (DRG) neurons are capable of firing at high frequencies, small unmyelinated DRG neurons typically exhibit much lower maximum firing frequencies. The molecular basis for this difference has not been delineated. Voltage-gated sodium channels play a critical role in excitable cells including DRG neurons, because they underlie the depolarizing phase of action potentials which these cells use to transmit information, and may contribute to subthreshold currents that influence action potential electrogenesis. As might be expected from the different firing properties of different types of neurons, the voltage-dependent and kinetic properties of sodium currents recorded from different neuronal populations can show substantial differences (Raman & Bean, 1997; Cummins *et*

al. 2002). Recently we demonstrated that while the TTX-sensitive currents of large DRG neurons (which give rise to myelinated A-fibres (Harper & Lawson, 1985) and can follow firing frequencies of > 100 Hz (Waddell & Lawson, 1990)) exhibit rapid repriming, i.e. fast recovery from inactivation (Everill *et al.* 2001), the TTX-sensitive currents of small DRG neurons (which give rise to unmyelinated or lightly myelinated axons and can follow significantly lower frequencies, e.g. ~16 Hz, of stimulation (Waddell & Lawson 1990)) exhibit slow recovery from inactivation (Elliott & Elliott, 1993; Cummins & Waxman, 1997; Black *et al.* 1999). This suggests that the repriming rate of sodium channels may be an important determinant of maximum following frequency.

At least nine distinct voltage-gated sodium channels have been cloned from mammals (Black & Waxman, 1996; Goldin *et al.* 2000). Many of these channels have specific

developmental, tissue or cellular distributions (Felts *et al.* 1997), and expression of recombinant channels in *Xenopus* oocytes and mammalian cells indicates that the different channels can have distinct kinetic and voltage-dependent properties (Smith & Goldin, 1998; Cummins *et al.* 1998, 2001). Interestingly, the $Na_V1.7$ sodium channel, which is highly expressed in small DRG neurons (Gould *et al.* 2000; Djouhri *et al.* 2003), shows slow repriming kinetics when expressed in HEK293 cells (Cummins *et al.* 1998). $Na_V1.7$ also displays slow onset of closed-state inactivation, a feature which permits it to respond to small, slow depolarizations (Cummins *et al.* 1998) and which may be relevant to its deployment at or close to sensory nerve terminals (Toledo-Aral *et al.* 1997). $Na_V1.6$ (previously termed NaCh6 or Scn8a) is highly expressed in large DRG neurons while small DRG neurons express low levels of message for this isoform (Black *et al.* 1996). Several studies have indicated that $Na_V1.6$ is the predominant isoform located at mature nodes of Ranvier (Caldwell *et al.* 2000; Krzemien *et al.* 2000; Boiko *et al.* 2001) along myelinated axons, which are notable for not firing in response to slow depolarizations but do fire in response to rapid depolarizations and are capable of following high-frequency stimulation (Kocsis *et al.* 1983). However, the repriming kinetics of $Na_V1.6$ channels have not thus far been characterized.

In the present study, we hypothesized that, in order to support conduction of high-frequency impulse trains along myelinated axons, $Na_V1.6$ channels would display rapid repriming and, because of their complementary patterns of deployment in large and small DRG neurons, we compared $Na_V1.6$ and $Na_V1.7$ sodium currents. Because the properties of sodium currents can depend on the cells in which they are expressed (Cummins *et al.* 2001), we characterized $Na_V1.6$ and $Na_V1.7$ channels expressed within DRG neurons. Our results show that $Na_V1.6$ and $Na_V1.7$ TTX-sensitive sodium channels have distinct repriming and closed-state inactivation properties. These differences may be important determinants of the integrative and firing properties of DRG sensory neurons.

METHODS

Construction of mammalian expression vectors encoding neuronal rat $Na_V1.6$ channel

These studies utilized a cDNA construct that encodes the mouse $Na_V1.6$ open reading frame. This construct varies from the original published mouse sequence (Burgess *et al.* 1995) at several nucleotides as reported by Smith *et al.* (1998). The complete open reading frame of mouse $Na_V1.6$, which was generously provided by Dr A. Goldin (University of California, Irvine), was excised from a pLCT1 oocyte expression vector by digestion first with AatII, then blunting the ends with T4 DNA polymerase, followed by digestion with *Xho*I to release the $Na_V1.6$ insert. A mammalian expression vector pcDNA3.1 (Invitrogen), modified to render it a low copy vector (Klugbauer *et al.*1995), was digested with *Apa*I,

the ends were blunted with T4 DNA polymerase, and it was then digested with *Xho*I. In a subsequent ligation reaction the two DNA pieces were joined to form a 13 kb plasmid. Isolates that displayed the expected digestion pattern using *Bam*HI were verified by sequencing the entire $Na_V1.6$ insert.

For expression within DRG neurons, a TTX-resistant (TTX-R) derivative of $Na_V1.6$ ($Na_V1.6r$) was produced by converting tyrosine 371 to serine (Y371S) as previously described for the $Na_V1.3$ channel (Cummins *et al.* 2001). Similarly, a TTX-R derivative of $Na_V1.7$ ($Na_V1.7r$) was produced by converting tyrosine 362 to serine (Y362S). These point mutations were introduced into the channel sequence using the Quick Change XL mutagenesis kit (Stratagene) with two mutagenic primers designed according to the manufacturer's instructions. The mutant constructs were subsequently verified by sequencing.

Culture of DRG neurons

DRG neurons were cultured from mice following a protocol approved by the Yale Animal Care and Use Committee. Mice were rendered unconscious by exposure to CO_2 and decapitated. DRG neurons were cultured as described previously (Caffrey *et al.* 1992). Briefly, the L4 and L5 DRGs were harvested from adult $Na_V1.8$-null mice (Akopian *et al.* 1999). The DRGs were treated with collagenase A (1 mg ml^{-1}) for 25 min, and collagenase D (1 mg ml^{-1}) and papain (30 u ml^{-1}) for 25 min, dissociated in Dulbeccos's modified Eagle's medium and Ham's F12 medium supplemented with 10 % fetal bovine serum, and plated on glass coverslips. $Na_V1.8$-null neurons were kept under standard tissue culture conditions for 5–7 days before biolistic transfections. We previously showed that $Na_V1.8$-null DRG neurons do not express fast- or slow-inactivating TTX-R sodium currents (Cummins *et al.* 1999, 2001). Some $Na_V1.8$-null DRG neurons do express persistent TTX-R sodium currents (Cummins *et al.* 1999), but these currents typically display amplitudes < 1 nA after several days in culture and run down quickly in the whole-cell recording configuration; therefore these persistent TTX-R currents are not significant under the culture and recording conditions used in the present study.

Biolistic transfection of $Na_V1.8$-null DRG neurons

The Helios Gene Gun System (Bio-Rad Laboratories) was used for biolistic transfection of neurons (Wellmann *et al.* 1999). $Na_V1.6r$ or $Na_V1.7r$ DNA (10 μg) was mixed with 5 μg green fluorescent protein (GFP) DNA and biolistic cartridges were made as described previously (Cummins *et al.* 2001) using 1.6 μm gold particles. Immediately prior to biolistic transfection, the culture medium was removed from the Petri dish. The gene gun was held ~2 cm above the cells and a pressure of ~120 p.s.i. (~827 kPa) was used to discharge the gold particles. Within 24 h the cells usually showed expression of GFP, indicating a successful biolistic transfection. Electrophysiological studies were conducted 18–48 h after transfection and most of the cells that expressed GFP also expressed fast-inactivating TTX-resistant sodium currents. Since these currents are not observed in untransfected $Na_V1.8$-null neurons or $Na_V1.8$-null neurons transfected with GFP alone, this confirmed that most of the cells that expressed GFP had also been successfully cotransfected with the $Na_V1.6r$ or $Na_V1.7r$ DNA.

Whole-cell patch-clamp recordings

Whole-cell patch-clamp recordings were conducted at room temperature (~21 °C) using a HEKA EPC-9 amplifier. Data were acquired on a Windows-based Pentium-III computer using the Pulse program (v 8.1, HEKA Electronic, Germany). Fire-polished

electrodes (0.8–1.5 MΩ) were fabricated from 1.7 mm capillary glass using a Sutter P-97 puller (Novato, CA, USA). To optimize space clamp, only isolated cells with a soma diameter of less than 30 μm were selected for recording. Cells were not considered for analysis if the initial seal resistance was less than 2 GΩ, if they had high leakage currents (holding current > 0.5 nA for DRG neurons), or an access resistance greater than 4 MΩ. The average access resistance was 1.8 ± 0.6 MΩ (mean ± S.D., $n = 82$). Voltage errors were minimized using 80–90 % series resistance compensation and the capacitance artifact was cancelled using the computer-controlled circuitry of the patch-clamp amplifier. Linear leak subtraction, based on resistance estimates from either four or five hyperpolarizing pulses applied before the depolarizing test potential, was used for all voltage-clamp recordings. Membrane currents were usually filtered at 5 kHz and sampled at 20 kHz. The pipette solution contained (mM): 140 CsF, 1 EGTA, 10 NaCl and 10 Hepes (pH 7.3). The standard bathing solution was (mM): 140 NaCl, 3 KCl, 1 $MgCl_2$, 1 $CaCl_2$, 0.05 $CdCl_2$, and 10 Hepes (pH 7.3). The liquid junction potential for these solutions was < 8 mV; data were not corrected to account for this offset. The osmolarity of all solutions was adjusted to 310 mosmol l^{-1} (Wescor 5500 osmometer, Logan, UT, USA). The offset potential was zeroed before patching the cells.

Data analysis

Data were analysed using the Pulsefit (HEKA Electronic, Germany) and Origin (OriginLab Corp., Northampton, MA, USA) software programs. Unless otherwise noted, statistical significance was determined by $P < 0.05$ using Student's unpaired t test. Results are presented as means ± S.E.M. and error bars in the figures represent the S.E.M. The curves in the figures are drawn by eye unless otherwise noted. Time course data were fitted with single exponential functions.

RESULTS

Robust expression of Na_v1.6r and Na_v1.7r currents in Na_v1.8-null DRG neurons

Because we were interested in the properties of Na_v1.6 and Na_v1.7 currents in DRG neurons, we expressed Na_v1.6 and Na_v1.7 channels directly in DRG neurons. In order to identify the Na_v1.6 and Na_v1.7 currents against the background of other TTX-sensitive sodium currents in DRG neurons, Na_v1.6 and Na_v1.7 channels were made TTX resistant (TTX-R) by replacing the tyrosine at a critical position for TTX binding (Sivilotti *et al.* 1997; Cummins *et al.* 2001) with a serine, and these TTX-R channels (referred to as Na_V1.6r and Na_v1.7r) were expressed in cultured DRG neurons from Na_v1.8-null mice. These neurons, which lack functional Na_v1.8 slow-inactivating TTX-R sodium currents and express very low levels of persistent TTX-R sodium current after several days in culture, provide a mammalian neuronal expression system in which other sodium channels, mutated to become TTX-R, can be studied in isolation (Cummins *et al.* 2001). Na_v1.8-null DRG neurons in culture for 5–7 days were transfected with GFP alone or in combination with Na_v1.6r or Na_v1.7r. Sodium currents were recorded in the presence of 500 nM TTX, 24–48 h after transfection. No TTX-R sodium

currents were observed in Na_v1.8-null neurons transfected with GFP alone (peak amplitude 0.22 ± 0.04 nA, $n = 20$). By contrast, the Na_v1.6r and Na_v1.7r channels produced large fast-inactivating TTX-R sodium currents (Fig. 1*A* and *B*). The average peak current amplitude was 29.9 ± 3.8 nA ($n = 46$) for Na_v1.6r currents and 29.5 ± 8.3 nA ($n = 12$) for Na_v1.7r currents. The majority of DRG neurons recorded from were small (soma diameter < 30 μm) and the average cell capacitance was 22 ± 1 pF.

Voltage dependence of activation and steady-state inactivation

The largest peak sodium current amplitude recorded from the Na_v1.6r transfected DRG neurons was 101 nA. Endogenous TTX-sensitive sodium currents in DRG neurons can also be greater than 100 nA, but currents this large can be difficult to adequately voltage clamp. By using low resistance pipettes and 80–90 % series resistance compensation we were able to achieve reasonable voltage clamp of cells expressing even 30 nA currents (Fig. 1*A* and *B*). For our characterization of the voltage-dependent and kinetic properties we focused on data from cells expressing lower peak current amplitudes to minimize the voltage errors. For Fig. 1 we averaged data from 16 Na_v1.6r transfected cells (8.1 ± 1.3 nA) and eight Na_v1.7r transfected cells (13.9 ± 3.7 nA). The average access resistance in these cells was 1.8 ± 0.1 MΩ and the estimated maximum voltage error after series resistance compensation was 3.3 ± 0.6 mV. The current–voltage relationships for Na_v1.6r and Na_v1.7r currents are shown in Fig. 1*C*. The midpoint for voltage-dependent activation was -18.7 ± 1.4 mV and the slope value was 7.7 ± 0.3 for Na_v1.6r. The midpoint for voltage-dependent activation was -27.3 ± 2.1 mV and the slope value was 6.2 ± 0.8 for Na_v1.7r. The midpoint values were significantly different ($P < 0.05$). The steady-state inactivation curves, measured with 500 ms depolarizing prepulses, are shown in Fig. 1*D*. The midpoint of steady-state inactivation was -64.1 ± 1.7 mV and the slope factor was 7.0 ± 0.4 for Na_v1.6r; and they were -71.3 ± 2.4 mV and 6.8 ± 0.4 for Na_v1.7r. The midpoints of inactivation were significantly different ($P < 0.05$). The currents elicited by step depolarizations ranging from -40 to $+40$ mV were fitted using a m^3h Hodgkin and Huxley (1952) model to estimate the time constants for activation (Fig. 1*E*) and fast inactivation (Fig. 1*F*). The kinetics of activation and fast inactivation were not significantly different ($P > 0.05$) for Na_v1.6r and Na_v1.7r currents.

Recovery from inactivation

Large and small cutaneous afferent DRG sensory neurons display dramatic differences in the repriming kinetics of their TTX-sensitive sodium currents (Everill *et al.* 2001). While the TTX-sensitive sodium currents in small DRG neurons reprime slowly (τ ~90 ms at -80 mV), the repriming of TTX-sensitive sodium currents in large DRG

neurons is fast (τ ~12 ms at −80 mV). We were interested in comparing the repriming kinetics of Na$_v$1.6, which is expressed at higher levels in large, compared to small, DRG neurons (Black *et al.* 1996), and Na$_v$1.7, which is more highly expressed in small DRG neurons (Gould *et al.* 2000; Djouhri *et al.* 2003).
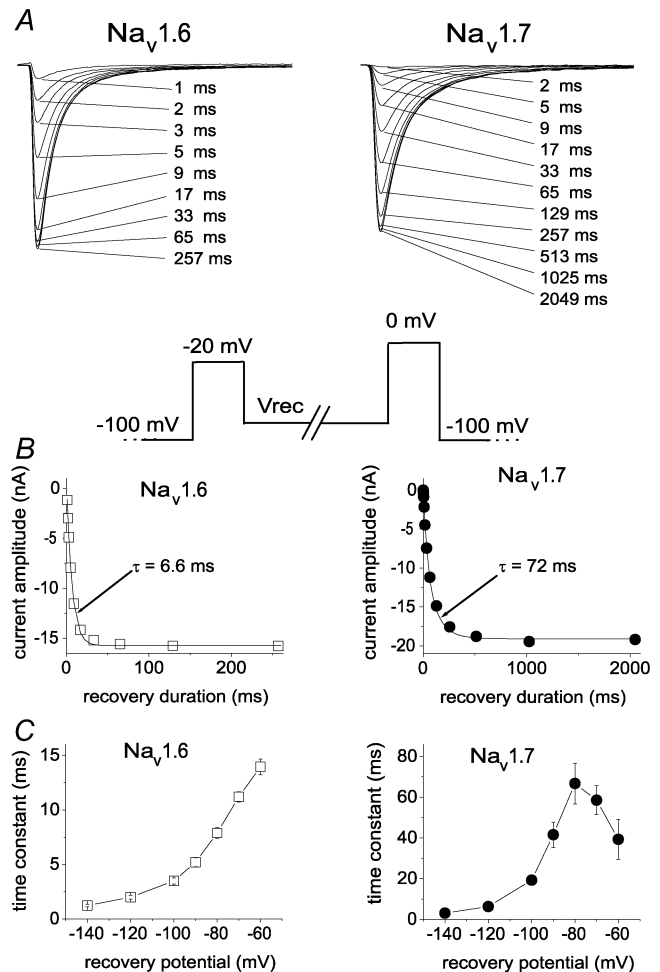
The repriming kinetics of Na$_v$1.6r channels expressed in DRG neurons were fast (τ ~8 ms at −80 mV; Fig. 2*A* and *B*, left). The repriming kinetics of Na$_v$1.6r currents were measured at recovery voltages from −140 to −60 mV and single exponential fits were used to estimate the repriming time constants that are shown in Fig. 2*C* (left). By contrast the repriming kinetics of Na$_v$1.7r channels expressed in

DRG neurons were slow (τ ~ 70 ms at −80 mV; Fig. 2*A* and *B*, right). The repriming time constants of Na$_v$1.7r currents estimated at recovery voltages from −140 to −60 mV are shown in Fig. 2*C* (right).
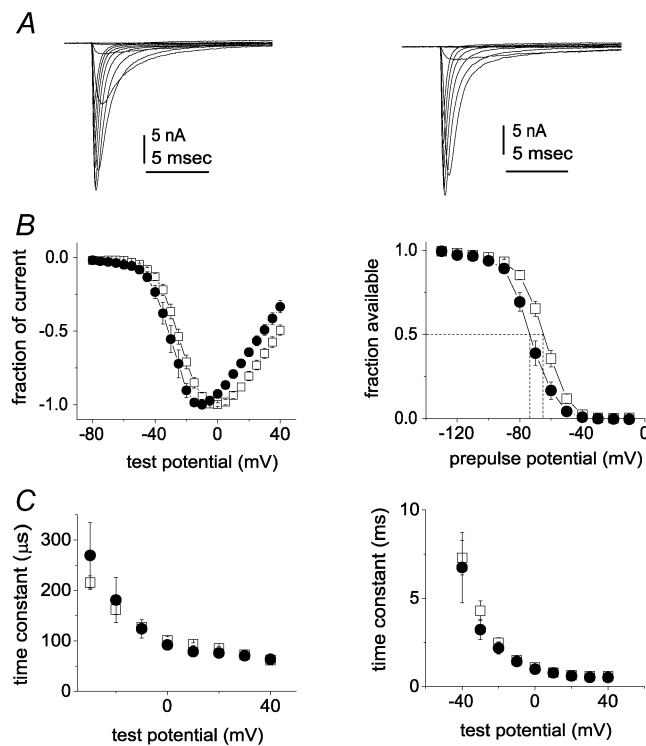
Figure 1. Comparison of Na$_v$1.6r and Na$_v$1.7r current properties

Representative traces from Na$_v$1.8-null DRG neurons expressing Na$_v$1.6r channels (*A*) and Na$_v$1.7r channels (*B*) are shown. The currents were elicited by 50 ms test pulses to various potentials from −80 to 40 mV. Cells were held at −120 mV. *C,* normalized peak current–voltage relationship for Na$_v$1.6r (□; n = 16) and Na$_v$1.7r channels (●; n = 10). *D*, voltage dependence of Na$_v$1.6r (□; n = 16) and Na$_v$1.7r (●; n = 12) sodium current steady-state inactivation. Steady-state inactivation was estimated by measuring the peak current amplitude elicited by 20 ms test pulses to 0 mV after 500 ms prepulses to potentials over the range of −130 mV to −10 mV. Current is plotted as a fraction of the maximum peak current. *E*, activation time constants as a function of voltage are shown for Na$_v$1.6r (□; n = 14) and Na$_v$1.7r (●; n = 7) currents in Na$_v$1.8-null DRG neurons. *F*, inactivation time constants are shown for Na$_v$1.6r (□; n = 14) and Na$_v$1.7r (●; n = 7) currents in Na$_v$1.8-null DRG neurons as a function of voltage. The activation and inactivation time constants were estimated from Hodgkin-Huxley m^3h fits to the currents elicited by 50 ms step depolarizations to voltages ranging from −40 to +40 mV.

Figure 2. Repriming (recovery from inactivation) kinetics are much faster for Na$_v$1.6r than Na$_v$1.7r channels in Na$_v$1.8-null DRG neurons

*A*, family of current traces from representative neurons expressing Na$_v$1.6r channels (left) and Na$_v$1.7r channels (right) showing the rate of recovery from inactivation at −80 mV. The standard repriming voltage protocol is shown below. The cells were prepulsed to −20 mV for 20 ms to inactivate all of the current, then brought back to the recovery potential (V_{rec}) for increasing recovery durations prior to the test pulse to 0 mV. The maximum pulse rate was 0.5 Hz. The times indicated for each trace shown in *A* correspond to the recovery duration for that trace. *B*, the time course for recovery from inactivation of peak Na$_v$1.6r (left) and Na$_v$1.7r (right) currents in *A* are shown (note different time scales on *x*-axes). The continuous curve is a single exponential function fitted to the data, with a time constant τ of 6.6 ms for the Na$_v$1.6r currents and 72 ms for the Na$_v$1.7r currents. *C*, the time constants for recovery from inactivation of Na$_v$1.6r (left) and Na$_v$1.7r (right) currents are shown plotted as a function of voltage (note different time scales on *y*-axes). Time constants were estimated from single exponential fits to time courses measured at recovery potentials ranging from −140 to −60 mV with the protocol shown in *A* for currents recorded from neurons transfected with Na$_v$1.6r channels (n = 15) or Na$_v$1.7r channels (n = 11).

Figure 3 compares the repriming time constants of Na$_v$1.6r and Na$_v$1.7r currents to those of native TTX-sensitive currents measured in large cutaneous afferent DRG neurons and small DRG neurons. The Na$_v$1.6r repriming kinetics are similar to those of TTX-sensitive currents in large DRG neurons and the Na$_v$1.7r repriming kinetics are similar to those measured in small DRG neurons.

We used the same inactivating prepulse (20 ms at −20 mV) to examine the repriming kinetics of both Na$_v$1.6 and Na$_v$1.7. This is the same protocol that was used to examine the repriming kinetics of the native TTX-sensitive sodium currents in this and previous (Black *et al.* 1999; Everill *et al.* 2001) studies. More than 99.8 % of Na$_v$1.6 and Na$_v$1.7 current is inactivated at −20 mV under steady-state conditions (Fig. 1*D*) and, because the time constant for fast inactivation is ~2–2.5 ms at −20 mV (Fig. 1*F*), more than 97 % of Na$_v$1.6 and Na$_v$1.7 current is inactivated after 20 ms at −20 mV. The 20 ms inactivating prepulse at −20 mV should therefore be sufficient to induce fast inactivation without inducing significant slow inactivation. However, to test for the possibility that stronger inactivating prepulses might affect the repriming kinetics, we also examined the repriming kinetics of Na$_v$1.6 currents following a 20 ms inactivating prepulse to +20 mV and a 50 ms inactivating prepulse to −20 mV (Fig. 4*A*). The repriming kinetics of Na$_v$1.6 currents were similar with all three inactivating prepulses (Fig. 4*B*). Similarly, the repriming kinetics of Na$_v$1.7 currents were not affected by these different inactivating prepulses (data not shown). These data support the conclusion that Na$_v$1.6 and Na$_v$1.7 currents exhibit substantially different time courses for recovery from fast inactivation.

Development of closed-state inactivation

We have previously demonstrated that Na$_v$1.7 channels exhibit fivefold slower closed-state inactivation than Na$_v$1.4 channels in HEK293 cells, and we suggested that
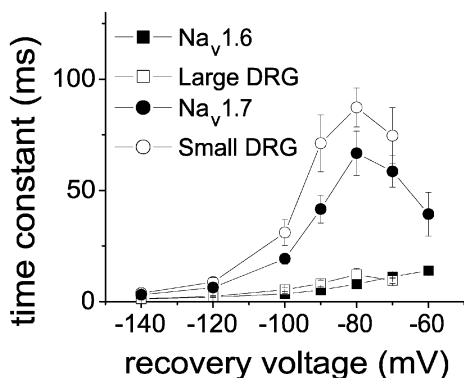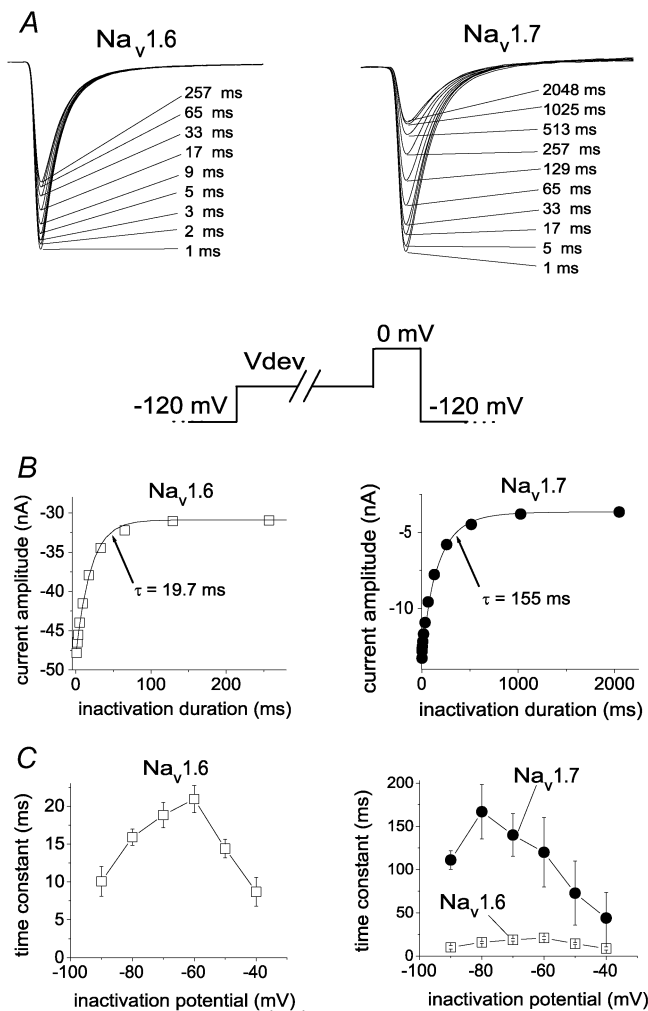
Figure 3

The recovery time constants for Na$_v$1.6r (■) and Na$_v$1.7r channels (●) expressed in Na$_v$1.8-null DRG neurons are compared to those for TTX-sensitive currents in large DRG neurons (□; from Everill *et al.* 2001) and TTX-sensitive currents in small DRG neurons (○; from Cummins *et al.* 1998).

differences in closed-state inactivation might contribute to the firing properties of neurons (Cummins *et al.* 1998). The closed-state inactivation kinetics of Na$_v$1.6 channels have not previously been characterized. Therefore we compared the development of inactivation kinetics of Na$_v$1.6r and Na$_v$1.7r channels in Na$_v$1.8-null neurons. At −70 mV, the development of inactivation was rapid (τ ~20 ms) for Na$_v$1.6r channels (Fig. 5*A* and *B*, left), but slow (τ ~150 ms) for Na$_v$1.7r channels (Fig. 5*A* and *B*, right). The time constant for development of inactivation was estimated at voltages ranging from −90 to −40 mV and
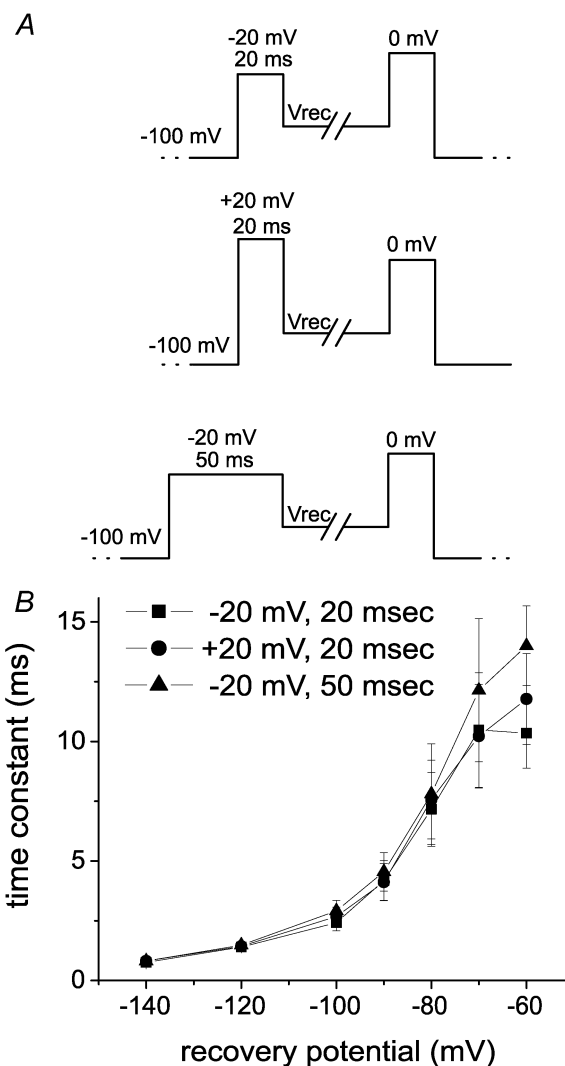
Figure 4. Recovery time constants for Na$_v$1.6r channels are not altered by changes in the inactivating prepulse

A, the three different inactivating prepulses used to examine the repriming kinetics of Na$_v$1.6r channels are shown. *B*, the repriming time constants measured with the different protocols for Na$_v$1.6r channels are shown. The first protocol used a 20 ms prepulse to −20 mV (■), the second protocol used a 20 ms prepulse to +20 mV (●) and the third protocol used a 50 ms prepulse to −20 mV (▲) to inactivate the Na$_v$1.6r channels. The repriming kinetics were always fast for Na$_v$1.6r channels and were not altered by the use of different inactivating prepulses.

Figure 5. Development of closed-state inactivation is more rapid for Na$_v$1.6r than for Na$_v$1.7r channels expressed in Na$_v$1.8-null DRG neurons

A, family of current traces showing the rate of development of inactivation for Na$_v$1.6r channels (left) and Na$_v$1.7r channels (right) at −70 mV. The standard development of inactivation voltage protocol is shown below. From a holding potential of −120 mV, the cells were prepulsed to −70 mV (V_{dev}) for increasing durations, then stepped to 0 mV to determine the fraction of current inactivated during the prepulse. The duration of the inactivation prepulse for each data trace is indicated. *B*, time course for development of inactivation for the peak currents for Na$_v$1.6r and Na$_v$1.7r in *A* are shown. The continuous curve is a single exponential function fitted to the data, with a time constant of 19.7 ms for Na$_v$1.6r channels (left) and 155 ms for Na$_v$1.7r channels (right). *C*, the time constants for development of inactivation are shown plotted as a function of voltage. Time constants were estimated from single exponential fits to time courses measured at recovery potentials ranging from −90 to −40 mV with the protocol shown in *A* for currents recorded from neurons transfected with Na$_v$1.6r channels (□, left and right; *n* = 14) and neurons transfected with Na$_v$1.7r channels (●, right; *n* = 11). As can be seen in the right panel, the development of inactivation time constants for Na$_v$1.6r currents was much faster than for Na$_v$1.7 currents.

was relatively small throughout this voltage range for Na$_v$1.6r channels expressed in Na$_v$1.8-null DRG neurons (Fig. 5*C*, left) but relatively large for Na$_v$1.7r channels (Fig. 5*C*, right).

Characterization of subthreshold ramp currents

Previously we demonstrated that Na$_v$1.7 channels expressed in HEK293 cells generate larger currents in response to slow ramp depolarizations than Na$_v$1.4 (skeletal muscle) sodium channels. Like Na$_v$1.6r channels, Na$_v$1.4 channels exhibit fast recovery from inactivation and fast development of closed-state inactivation. Therefore we also measured the currents produced in Na$_v$1.8-null neurons in response to slow ramp depolarizations (−100 mV to +30 mV over 500 ms). These ramp depolarizations elicited smaller inward currents in Na$_v$1.8-null DRG neurons transfected with Na$_v$1.6r channels (Fig. 6*A*) than with Na$_v$1.7r channels (Fig. 6*B*). Because TTX was included in the bath, endogenous TTX-sensitive currents were blocked. The relative ramp current amplitude (normalized to peak current amplitude) elicited with this protocol averaged 1.4 ± 0.2 % (*n* = 37) for Na$_v$1.6r channels and 2.4 ± 0.4 % (*n* = 9) for Na$_v$1.7r channels (Fig. 6*C*) and this difference was significant (*P* < 0.05).

DISCUSSION

We have characterized the kinetic and voltage-dependent properties of the currents conducted by neuronal Na$_v$1.6 and Na$_v$1.7 sodium channels expressed in Na$_v$1.8-null DRG neurons. These channels produced large fast-activating and inactivating currents following biolistic transfection of cultured Na$_v$1.8-null DRG neurons. The Na$_v$1.6 currents were distinct from the currents generated by other TTX-sensitive neuronal sodium channels that we have studied in mammalian cells. Our data provide insights into how sodium currents and firing properties in neurons can be regulated by altering the underlying sodium channel α-subunits that are expressed.

### Comparison of Na$_v$1.6 to other voltage-gated sodium channels

Voltage-dependent sodium currents underlie the rapid upstroke of the action potential in neurons. At least eight different voltage-gated sodium channel α-subunits have been detected in neurons and many neuronal cell types have been shown to express more than one α-subunit. While the roles of these different α-subunits in electro-genesis are not yet fully understood, it is clear that different α-subunits can have distinct voltage-dependent and kinetic properties. TTX-R neuronal isoforms have very distinctive properties and exhibit major differences in their activation and inactivation kinetics and voltage dependence (Akopian *et al.* 1996; Cummins *et al.* 1999; Dib-Hajj *et al.* 2002). The differences between the TTX-sensitive channels have been more difficult to elucidate.

We show here that midpoints of the voltage dependence of activation and inactivation are 7–9 mV more positive for Na$_v$1.6 than for Na$_v$1.7 channels in DRG neurons. The comparable shifts in the voltage dependence of activation and steady-state inactivation are consistent with the hypothesis that activation and fast inactivation are coupled (Chahine *et al.* 1994).

We have also found that the different sodium channel isoforms exhibit substantial differences in recovery from inactivation. The time constant for recovery from inactivation for Na$_v$1.6r channels at −80 mV is ~10-fold faster than that for Na$_v$1.7r channels and 2-fold faster than that for Na$_v$1.3r channels expressed in DRG neurons (Cummins *et al.* 2001). Na$_v$1.6 is the major sodium channel at nodes of Ranvier (Caldwell *et al.* 2000), and myelinated axons are known to follow high-frequency stimulation (Kocsis *et al.* 1983). Since repriming kinetics may help determine how fast a neuron can repetitively fire, this suggests that membranes expressing Na$_v$1.6 channels should be able to sustain higher firing rates than membranes expressing Na$_v$1.7 channels. Although Na$_v$1.7 and Na$_v$1.6 channels exhibit substantially different repriming kinetics, and our data suggest that this reflects recovery from the fast-inactivated state for both isoforms, it is not clear which channel structures account for this difference. Although the amino acid sequences of these two isoforms are well conserved (Goldin *et al.* 2000), the sequences differ in many places, especially in the loops that join the transmembrane segments.

Development of closed-state inactivation is also much faster for Na$_v$1.6r channels than for either Na$_v$1.7r or Na$_v$1.3r channels. At −70 mV, Na$_v$1.6r channels inactivated with a time constant of ~20 ms, compared to ~150 ms for Na$_v$1.7r channels (see Fig. 5*C*) and ~120 ms for Na$_v$1.3 channels (Cummins *et al.* 2001). These data indicate that the rate of transitions between the closed-inactivated and closed states is significantly slower for Na$_v$1.7 than Na$_v$1.6 channels. This suggests that cells expressing Na$_v$1.3 and Na$_v$1.7 channels may generate more robust responses to slowly depolarizing inputs than cells expressing Na$_v$1.6 channels, because Na$_v$1.3 and Na$_v$1.7 channels are less likely to undergo closed-state inactivation during slow depolarizations. Previously we proposed (Cummins *et al.* 1998) that slow closed-state inactivation of sodium currents can contribute to the development of large ramp currents. Indeed, the ramp currents generated by Na$_v$1.6 channels (~1.4 % of peak current amplitude) were smaller than Na$_v$1.7 ramp currents (~2.4 % of peak current amplitude) and Na$_v$1.3 ramp currents (4–7 % of peak current amplitude; Cummins *et al.* 2001). The voltage ramps that we employed, ~0.26 mV ms^{-1}, were designed to mimic slow depolarizations that could be caused by natural stimuli such as generator potentials and postsynaptic potentials. Our data indicate that Na$_v$1.3 and

Na$_v$1.7, which generated larger ramp currents, might be better than Na$_v$1.6 at boosting slow depolarizing inputs to DRG sensory neurons. The attenuated response of Na$_v$1.6 to small, slow depolarizations might be advantageous at nodes of Ranvier (where Na$_v$1.6 is the major channel; Caldwell *et al.* 2000), since nodes act as repeaters, generating action potentials in response to the large, rapid depolarizations produced by firing of upstream nodes. Kocsis *et al.* (1983) showed that, while myelinated axons follow high-frequency stimulation, they do not fire in response to sustained or slow depolarizations. However, studies on the sodium currents in cerebellar Purkinje neurons from Na$_v$1.6 knockout mice indicate that Na$_v$1.6 underlies a significant proportion of the subthreshold ramp currents in these neurons (Raman *et al.* 1997) and
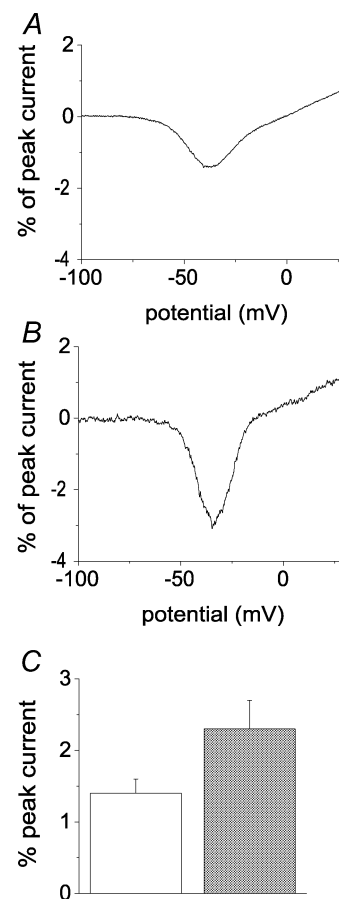
Figure 6. Ramp currents generated by Na$_v$1.6r and Na$_v$1.7r channels

A, representative current elicited in a Na$_v$1.8-null DRG neuron expressing Na$_v$1.6r channels by a 500 ms ramp depolarization from −100 to +30 mV is shown. The peak sodium current amplitude elicited in this cell with step depolarizations was 65.1 nA. *B*, representative current elicited in a Na$_v$1.8-null DRG neuron expressing Na$_v$1.7r channels by a 500 ms ramp depolarization from −100 to +30 mV is shown. The peak sodium current amplitude elicited in this cell with step depolarizations was 75.4 nA. *C*, The relative ramp current amplitude was significantly larger in cells expressing Na$_v$1.7r channels (grey bar) than in cells expressing Na$_v$1.6r channels (open bar).

the relative ramp current amplitude produced by Na$_v$1.6r channels in DRG neurons was quite variable, ranging from 0.2 to 4.5% of the peak current amplitude. These observations suggest that cellular factors may be able to modulate the Na$_v$1.6 ramp current amplitude in neurons. Strupp *et al.* (1992) reported that the reducing agent glutathione could influence sodium channel inactivation in rat axonal membrane patches, indicating that redox processes, possibly altered by changes in the metabolic state of axons, might modulate the gating of axonal sodium channels and also influence the firing properties of axons.

A ramp current, while relatively small, was detectable in all cells expressing Na$_v$1.6r that we studied. Because the density of sodium channels at the node is high ($> 10^3$ μm^{-2}; Ritchie & Rogart, 1977; Caffrey *et al.* 1992) it is possible that Na$_v$1.6 channels provide the persistent current that has been shown (Stys *et al.* 1993) to drive damaging reverse Na$^+$–Ca^{2+} exchange in myelinated axons after energy failure is induced by anoxia (Stys *et al.* 1992). Consistent with this hypothesis, the expression of Na$_v$1.6 channels is downregulated in demyelinated CNS axons (Craner *et al.* 2003), and it is known that sensitivity to anoxic injury is decreased in these axons following demyelination (Imaizumi *et al.* 1998). The relatively small magnitude of the ramp currents produced by Na$_v$1.6 may in fact be adaptive at nodes since the presence of other isoforms such as Na$_v$1.7, which produce larger ramp currents, might increase the sensitivity of nodes to energy deprivation.

Interestingly, Craner *et al.* showed that a significant switch from Na$_v$1.6 to Na$_v$1.2 at nodes of Ranvier within the optic nerve of rats with experimental allergic encephalomyelitis (EAE), a model of multiple sclerosis. Although the properties of Na$_v$1.2 have not been characterized in neurons, O'Leary (1998) characterized Na$_v$1.2 channels expressed in HEK293 cells. Na$_v$1.2 channels displayed repriming and closed-state inactivation kinetics in HEK293 cells that are ~3-fold slower than that of the Na$_v$1.6r currents reported here. Axons with predominantly Na$_v$1.2 channels at their nodes might be less reliable in terms of following sustained high-frequency stimulation and more likely to fire in response to sustained or slow depolarizations. Thus a switch in isoform expression at nodes could also contribute to the abnormal firing associated with axonal pathologies.

Comparison to native DRG sodium currents

The TTX-sensitive sodium currents in large DRG neurons exhibit predominantly fast repriming kinetics (Everill *et al.* 2001) similar to those of Na$_v$1.6r currents. The TTX-sensitive currents in small DRG neurons, however, exhibit predominantly slow repriming kinetics similar to those of Na$_v$1.7r currents (Cummins *et al.* 1998), suggesting that the observed difference is due to a differential isoform expression pattern. Black *et al.* (1996) found that while the

majority of large DRG neurons (which give rise to myelinated axons; Harper & Lawson, 1985) express moderate to high mRNA levels for Na$_v$1.1 and Na$_v$1.6, the majority of small DRG neurons express a low level of message for these isoforms. On the other hand, studies with Na$_v$1.7-specific antibodies show more intense staining of small DRG neurons than large DRG neurons (Gould *et al.* 2000; Djouhri *et al.* 2003). Djouhri *et al.* (2003) reported that Na$_v$1.7 immunoreactivity is negatively correlated with somal cell size and conduction velocity. However, in contrast to Nav1.9 sodium channel protein, which is predominantly found in small nociceptive DRG neurons (Fang *et al.* 2002), Na$_v$1.7 immunoreactivity is found in both nociceptive and low-threshold mechano-receptive neurons (Djouhri *et al.* 2003). Although these results in combination with our data suggest that at least the somal currents in small DRG neurons might be predominantly generated by Na$_v$1.7 and those in large DRG neurons might be predominantly generated by Na$_v$1.6, the lack of isoform-specific blockers prevents direct testing of these hypotheses. Furthermore, the repriming characteristics of Na$_v$1.1 sodium channels have not been characterized in mammalian cells and therefore it is difficult to predict the contribution of this isoform to the firing properties of DRG neurons.

Conclusions

Our data show that Na$_v$1.6 sodium channels generate currents in mammalian cells that are distinct from other TTX-sensitive sodium channels in several ways. The substantially faster repriming of Nav1.6 may contribute to the capability of large DRG neurons to fire at high frequencies, while the rapid development of closed-state inactivation might attenuate the response to slow, small depolarizations at nodes of Ranvier which act as repeaters, generating impulses in response to the large rapid depolarizations produced by firing at upstream nodes, and might protect nodes from damaging persistent sodium influx under conditions of energy deprivation. The different kinetics of TTX-sensitive neuronal sodium channel isoforms such as Na$_v$1.3 (Cummins *et al.* 2001), Na$_v$1.6 (this study) and Na$_v$1.7 (this study and Cummins *et al.* 1998) suggest that selective expression of specific sodium channel isoforms can help tune the excitability and repetitive firing properties of neurons.

REFERENCES

Akopian AN, Sivilotti L & Wood JN (1996). A tetrodotoxin-resistant voltage-gated sodium channel expressed by sensory neurons. *Nature* **379**, 257–262.

Akopian AN, Souslova V, England S, Okuse K, Ogata N, Ure J, Smith A, Kerr BJ, McMahon SB, Boyce S, Hill R, Stanfa LC, Dickenson AH & Wood JN (1999). The tetrodotoxin-resistant sodium channel Na$_v$1.8 has a specialized function in pain pathways. *Nature Neurosci* **2**, 541–548.

Black JA, Cummins TR, Plumpton C, Chen YH, Hormuzdiar W, Clare JJ & Waxman SG (1999). Upregulation of a silent sodium channel after peripheral, but not central, nerve injury in DRG neurons. *J Neurophysiol* **82**, 2776–2785.

Black JA, Dib-Hajj S, McNabola K, Jeste S, Rizzo MA, Kocsis JD & Waxman SG (1996). Spinal sensory neurons express multiple sodium channel α-subunit mRNAs. *Brain Res Mol Brain Res* **43**, 117–132.

Black JA & Waxman SG (1996). Sodium channel expression: a dynamic process in neurons and non-neuronal cells. *Dev Neurosci* **18**, 139–52.

Boiko T, Rasband MN, Levinson SR, Caldwell JH, Mandel G, Trimmer JS & Matthews G (2001). Compact myelin dictates the differential targeting of two sodium channel isoforms in the same axon. *Neuron* **30**, 91–104.

Burgess DL, Kohrman DC, Galt J, Plummer NW, Jones JM, Spear B & Meisler MH (1995). Mutation of a new sodium channel gene, Scn8a, in the mouse mutant 'motor endplate disease'. *Nat Genet* **10**, 461–465.

Caldwell JH, Schaller KL, Lasher RS, Peles E & Levinson SR (2000). Sodium channel Na$_v$1.6 is localized at nodes of ranvier, dendrites, and synapses. *Proc Natl Acad Sci U S A* **97**, 5616–5620.

Caffrey JM, Eng DL, Black JA, Waxman SG & Kocsis JD (1992). Three types of sodium channels in adult rat dorsal root ganglion neurons. *Brain Res* **592**, 283–297.

Chahine M, George AL Jr, Zhou M, Ji S, Sun W, Barchi RL & Horn R (1994). Sodium channel mutations in paramyotonia congenita uncouple inactivation from activation. *Neuron* **12**, 281–294.

Craner MJ, Lo AC, Black JA & Waxman SG (2003). Abnormal sodium channel distribution in optic nerve axons in a model of inflammatory demyelination. *Brain* **126**, 1552–1561.

Cummins TR, Aglieco F, Renganathan M, Herzog R, Dib-Hajj SD & Waxman SG (2001). Na$_v$1.3 sodium channels: rapid repriming and slow closed-state inactivation display quantitative differences following expression in a mammalian cell line and in spinal sensory neurons. *J Neurosci* **21**, 5952–5961.

Cummins TR, Dib-Hajj SD, Black JA, Akopian AN, Wood JN & Waxman SG (1999). A novel persistent tetrodotoxin-resistant sodium current in small primary sensory neurons. *J Neurosci* **19**, RC43, 1–6.

Cummins TR, Dib-Hajj SD, Waxman SG & Donnelly DF (2002). Characterization and developmental changes of Na$^+$ currents of petrosal neurons with projections to the carotid body. *J Neurophysiol* **88**, 2993–3002.

Cummins TR, Howe JR & Waxman SG (1998). Slow closed-state inactivation underlies tetrodotoxin-sensitive ramp currents in HEK293 cells expressing hNE sodium channels and in dorsal root ganglion neurons. *J Neurosci* **18**, 9607–9619.

Cummins TR & Waxman SG (1997). Down-regulation of TTX-resistant sodium currents and upregulation of a rapidly repriming TTX-sensitive sodium current in small spinal sensory neurons after nerve injury. *J Neurosci* **17**, 3503–3514.

Dib-Hajj SD, Black JA, Cummins TR & Waxman SG (2002). NaN/Na$_v$1.9: a sodium channel with unique properties. *Trends Neurosci* **25**, 253–259.

Djouhri L, Newton R, Levinson SR, Berry CM, Carruthers B & Lawson SN (2003) Sensory and electrophysiological properties of guinea-pig sensory neurones expressing Na$_v$1.7 (PN1) Na$^+$ channel α-subunit protein. *J Physiol* **546**, 565–576.

Elliott AA & Elliott JR (1993). Characterization of TTX-sensitive and TTX-resistant sodium currents in small cells from adult rat dorsal root ganglia. *J Physiol* **463**, 39–56.

Everill B, Cummins TR, Waxman SG & Kocsis JD (2001). Sodium currents of large (Aβ-type) adult cutaneous afferent dorsal root ganglion neurons display rapid recovery from inactivation before and after axotomy. *Neuroscience* **106**, 161–169.

Fang X, Djouhri L, Black JA, Dib-Hajj SD, Waxman SG & Lawson SN (2002). The presence and role of the tetrodotoxin-resistant sodium channel Na(v)1.9 (NaN) in nociceptive primary afferent neurons. *J Neurosci* **22**, 7425–7433.

Felts PA, Yokoyama S, Dib-Hajj S, Black JA & Waxman SG (1997). Sodium channel alpha-subunit mRNAs I, II, III, NaG, Na6 and hNE (PN1): different expression patterns in developing rat nervous system. *Brain Res Mol Brain Res* **45**, 71–82.

Goldin AL, Barchi RL, Caldwell JH, Hofmann F, Howe JR, Hunter JC, Kallen RG, Mandel G, Meisler MH, Netter YB, Noda M, Tamkun MM, Waxman SG, Wood JN & Catterall WA (2000). Nomenclature of voltage-gated sodium channels. *Neuron* **28**, 365–368.

Gould HJ 3rd, Gould TN, England JD, Paul D, Liu ZP & Levinson SR (2000). A possible role for nerve growth factor in the augmentation of sodium channels in models of chronic pain. *Brain Res* **854**, 19–29.

Harper AA & Lawson SN (1985). Conduction velocity is related to morphological cell type in rat dorsal root ganglion neurones. *J Physiol* **359**, 31–46.

Hodgkin AL & Huxley AF (1952). A quantitative description of membrane current current and its application to conduction and excitation in nerve. *J Physiol* **117**, 500–544.

Imaizumi T, Kocsis JD & Waxman SG (1998). Resistance to anoxic injury in the dorsal columns of adult rat spinal cord following demyelination. *Brain Res* **779**, 292–296.

Klugbauer N, Lacinova L, Flockerzi V & Hofmann F (1995). Structure and functional expression of a new member of the tetrodotoxin-sensitive voltage-activated sodium channel family from human neuroendocrine cells. *EMBO J* **14**, 1084–1090.

Kocsis JD, Ruiz JA & Waxman SG (1983). Maturation of mammalian myelinated fibers: changes in action-potential characteristics following 4-aminopyridine application. *J Neurophysiol* **50**, 449–463.

Krzemien DM, Schaller KL, Levinson SR & Caldwell JH (2000). Immunolocalization of sodium channel isoform NaCh6 in the nervous system. *J Comp Neurol* **420**, 70–83.

O'Leary ME (1998). Characterization of the isoform-specific differences in the gating of neuronal and muscle sodium channels. *Can J Physiol Pharmacol* **76**, 1041–1050.

Raman IM & Bean BP (1997). Resurgent sodium current and action potential formation in dissociated cerebellar Purkinje neurons. *J Neurosci* **17**, 4517–4526.

Raman IM, Sprunger LK, Meisler MH & Bean BP (1997). Altered subthreshold sodium currents and disrupted firing patterns in Purkinje neurons of Scn8a mutant mice. *Neuron* **19**, 881–891.

Ritchie JM & Rogart RB (1977). Density of sodium channels in mammalian myelinated nerve fibers and nature of the axonal membrane under the myelin sheath. *Proc Natl Acad Sci U S A* **74**, 211–215.

Sivilotti L, Okuse K, Akopian AN, Moss S & Wood JN (1997). A single serine residue confers tetrodotoxin insensitivity on the rat sensory-neuron-specific sodium channel SNS. *FEBS Lett* **409**, 49–52.

Smith RD & Goldin AL (1998). Functional analysis of the rat I sodium channel in *Xenopus* oocytes. *J Neurosci* **18**, 811–820.

Smith MR, Smith RD, Plummer NW, Meisler MH & Goldin AL (1998). Functional analysis of the mouse Scn8a sodium channel. *J Neurosci* **18**, 6093–6102.

Strupp M, Quasthoff S, Mitrovic N & Grafe P (1992). Glutathione accelerates sodium channel inactivation in excised rat axonal membrane patches. *Pflugers Arch* **1421**, 283–285.

Stys PK, Sontheimer H, Ransom BR & Waxman SG (1993). Noninactivating, tetrodotoxin-sensitive Na$^+$ conductance in rat optic nerve axons. *Proc Natl Acad Sci U S A* **90**, 6976–6980.

Stys PK, Waxman SG & Ransom BR (1992). Ionic mechanisms of anoxic injury in mammalian CNS white matter: role of Na$^+$ channels and Na$^+$–Ca^{2+} exchanger. *J Neurosci* **12**, 430–439.

Toledo-Aral JJ, Moss BL, He Z-J, Koszowski AG, Whisenand T, Levinson SR, Wolf JJ, Silos-Santiago I, Halegoua S & Mandel G (1997). Identification of PN1, a predominant voltage-dependent sodium channel expressed principally in peripheral neurons. *Proc Natl Acad Sci USA* **94**, 1527–1532.

Waddell PJ & Lawson SN (1990). Electrophysiological properties of subpopulations of rat dorsal root ganglion neurons *in vitro*. *Neuroscience* **36**, 811–22.

Wellmann H, Kaltschmidt B & Kaltschmidt C (1999). Optimized protocol for biolistic transfection of brain slices and dissociated cultured neurons with a hand-held gene gun. *J Neurosci Methods* **92**, 55–64.

Acknowledgements